

Received 23 September 2022, accepted 14 November 2022, date of publication 17 November 2022, date of current version 22 November 2022.

Digital Object Identifier 10.1109/ACCESS.2022.3222820

RESEARCH ARTICLE

Dangerous Area of Tethered UAV Due to Impact

TAO YE¹, XU XIANGYU², AND DAI JIAXI³

¹Department of Mechanics, School of Mechanical Engineering, Tianjin University, Tianjin 300354, China

²Institute of Defense Engineering, AMS, PLA, Beijing 100850, China

³Architectural and Civil Engineering, School of Shenyang Urban Construction University, Shenyang 110121, China

Corresponding author: Tao Ye (taoye123@tju.edu.cn)

ABSTRACT Tethered UAV is composed of a UAV platform, tethered cable and winch. The UAV platform and tethered cable are an interactive whole, and the movement of the UAV platform will change the configuration and tension of the tethered cable. Under extreme external conditions (such as strong airflow) or unprofessional operation, the UAV platform will be prone to extreme movement, which will impact the tethered cable, and in serious cases, the tethered UAV will not work normally. To study the influence on the tethered UAV due to impact, equations for the relation between impact stress and impact parameters are derived and numerically solved to determine the dangerous area of the tethered UAV based on two failure criteria. The obtained results reveal that a smaller elastic modulus and cross-sectional area will lead to less failure of the tethered UAV, and the breaking strength of the cable is vital to the tethered UAV when it is impacted. Engineering suggestions are also provided to make tethered UAVs safer.

INDEX TERMS Tethered UAV, impact, dangerous area.

I. INTRODUCTION

Because of the clear advantages of static hovering and stability, UAVs have been widely used in resource exploration, anti-terrorism monitoring, civil aerial photography, and other fields. However, UAVs have the problem of poor endurance, and the information transmitted by UAVs wirelessly is also easily hijacked. Therefore, the UAV platform can be connected to an optoelectronic composite tether to make it work for a long time and ensure the efficiency and safety of information transmission. This type of UAV is called a tethered UAV.

Compared with ordinary UAVs, tethered UAVs have the advantages of long hovering times and abundant power and have broader application prospects. Due to these advantages, tethered UAVs are widely used in the fields of bridge safety detection [1], forest firefighting [2], and maritime emergency communication [3].

Ordinary UAVs and tethered UAVs mainly operate in low-altitude and ultralow-altitude environments. In this area, UAV platforms are vulnerable to various types of impacts, which will greatly affect their operation. Under the impact, the UAV

will not only greatly move but will also be damaged by the impact, which will greatly influence its operation. Various studies have mainly focused on the impact on ordinary UAVs. Chi Chen et al. conducted a numerical simulation of a UAV falling at different heights. He found that the heading angle, pitch angle, and velocity of the UAV during collision had a significant effect on the impact load between the UAV and the impacted object [4]. Akhilesh Kumar Jha et al. focused on the numerical modeling and simulation of a two-pound bird impact on composite structures of a UAV using ABAQUS/Explicit with impact velocities ranging from 40 m/s and 60 m/s [5]. Xiaohua Lu et al. analyzed the impact of birds and UAVs on aircraft head through finite element models, and the obtained results showed that for UAVs and birds of similar quality, the former would cause greater damage to the aircraft head [6]. Zhang et al. built a high-precision UAV model and verified the accuracy of the model through drop experiments. Then, he evaluated the impact process, possible damaged components, and failure modes of the UAV at different angles and speeds. The obtained results showed that under certain angles and speeds, the UAV would be irreparably damaged after being hit, and the UAV battery would be at risk of fire [7]. Eamon T et al. estimated the range of injury risks to humans due to the unmanned aerial system

The associate editor coordinating the review of this manuscript and approving it for publication was Rosario Pecora¹.

(UAS) impact, and live flight tests were observed to be less severe than falling impact tests [8]. Meng et al. simulated the dynamic response of the horizontal stabilizer during UAS airborne collision, and the obtained results showed that the UAV impact at the airliner cruising speed may cause some damage to the horizontal stabilizer front spar, in which the hardness of drone components rather than kinetic energy is a decisive factor [9]. Choon et al. presented a weight threshold study based on the impact of the drones on the human head, and the weight and height of the UAV are determined according to the energy required for a skull fracture, which provides a design basis for the UAV flying at a low altitude [10]. Hu Liu et al. not only studied the damage caused when the UAV collided with the aircraft engine but also considered the impact of the UAV debris on the engine after it was inhaled by the engine and judged the impact of the aircraft by the percentage of the engine thrust loss [11].

The power supply and information transmission of the tethered UAV depend on the photoelectric composite cable. Since the UAV platform and the tethered cable are an interactive whole, the movement of the UAV platform will affect the internal tension of the tethered cable. When the tension is too large, the tethered cable will be damaged, which will also lead to the failure of the tethered UAV. Therefore, it is not enough to only pay attention to the dynamic response of the UAV platform when it is impacted but also to consider the impact of the UAV platform on the tethered cable. Many experts have worked on the dynamic model and control rules to assure the tethered UAV's stable operation. When constructing the control algorithm for a ship-borne tethered UAV, Wu Y et al. simplified the tethered cable to the spring-mass-damping model, neglecting the cable's local bending [12]. Nicotra et al. concentrated on developing a stabilizing control law for an aerial aircraft connected to a base station by a taut cable [13]. Muttin evaluated the ship-borne tethered UAV system and constructed a nonlinear dynamic model, simplifying it [14]. Ya L et al. examined the dynamic available wrench set and maximum maneuver acceleration before optimizing UAV paths to keep the tethers taut [15]. Talke et al. considered the mission of a UAV tethered to a small unmanned surface vehicle (USV), extended the tether control reference model based on static catenary theory, and decoupled the dynamic motion of a USV from that of a UAV [16]. Wei H et al. performed a numerical analysis of the stability parameter range of tethered UAVs under the action of the transient wind field and provided some suggestions for the practical engineering design of tethered UAV systems [17]. O. M. Bushnaq et al. achieved the maximum cellular coverage of tethered UAVs in the user group and found that tethered UAVs outperformed ordinary UAVs, given that sufficient GS location accessibility and tether length were provided [18]. Ahmad Kourani et al. designed a novel robot system in which the UAV connected the buoy through cables and controlled the speed of the buoy [19]. Sandino et al. designed a scheme to connect an unmanned helicopter and the landing point with a tethered cable to ensure a smooth landing of the helicopter

[20]. These studies mainly focus on the dynamic response and control law of tethered UAVs under a stable wind field or slight disturbance, but there is no research on whether tethered UAVs can work stably under impact.

A photoelectric composite cable is an important difference between tethered and ordinary UAVs. In addition to the impact on the tethered UAV platform, the impact on the optoelectronic composite cable will also lead to the failure of the tethered UAV. This occurs because when the optoelectronic composite cable fails, the tethered UAV platform will encounter power failure and information transmission problems, which may lead to the crash of the tethered UAV in serious cases. Although there is no research on the dynamic response of the tethered UAV when it is impacted, many similar problems have been studied in other fields. Cable-supported structures were widely used in deep-water mooring, suspension bridges, and other fields. Some studies have focused on the robustness of such structures to highly transient loading conditions. One of the key problems was the damage or collapse of the whole structure caused by the sudden destruction of cables [21], [22], [23]. When studying the dynamic response of cable subjected to impact, the relationship between impact speed and impact force was often found because the impact speed is invariant in an instant [24]. Therefore, the main concern of this work is the impact on the tethered cable caused by the UAV platform. According to the two failure criteria to ensure the normal operation of the tethered UAV, the impact speed and angle that make the tethered UAV in the dangerous working area are given.

The remainder of the paper is organized as follows. In Section 2, the equations between the impact stress and impact parameters of the tethered UAV are derived. In Section 3, the conditions for failure of tethered UAV operation are given. In Section 4, the numerical simulation is performed to analyze the dangerous area of the tethered UAV due to impact. In Section 5, the engineering suggestions are given based on the numerical results and the actual working conditions. Finally, Section 6 concludes the paper.

II. THEORETICAL ANALYSIS

The tethered cable is fixed to the ground at its lower end and attached to the UAV at its upper end. The lower end of the tethered UAV is determined by what it tethers. For example, the lower end of a ship-borne tethered UAV or vehicle tethered UAV's motion is determined by the ship or vehicle, and the tethered UAV that tethers to the ground has a static lower end. The force diagram of the UAV is shown in Figure 1, and the boundary condition of the upper end is derived as follows:

where $o_b x_b z_b$ is the body coordinate system in the plane of the UAV, V_c is the horizontal wind speed, F is the total lift of the UAV, θ_0 is the inclination between $o_b x_b$ and the horizontal direction, $\theta^i(L)$ is the included angle between e_1 and the horizontal direction, Mg is the gravity of the UAV, P_t is the total tension of the cable to the tethered UAV, and F_{D_x} and F_{D_z} are the aerodynamic forces received by the UAV in

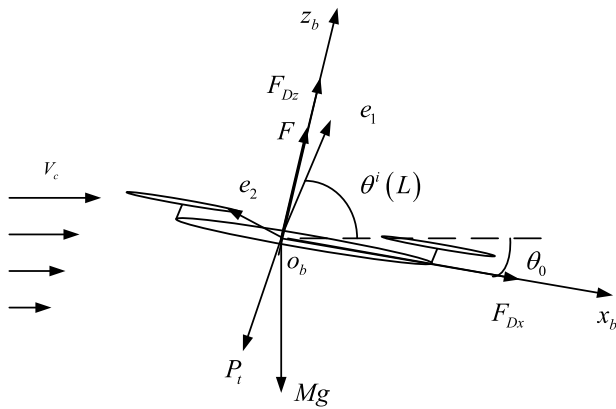


FIGURE 1. Force diagram of the UAV.

the $o_b x_b$ and $o_b z_b$ directions, respectively. The expression is:

$$F_{Dx} = \frac{1}{2} \rho_f C_{Dx} V_x |V_x| \quad (1)$$

$$F_{Dz} = \frac{1}{2} \rho_f C_{Dz} V_z |V_z| \quad (2)$$

where V_x is the component of V_c in $o_b x_b$, V_z is the component of V_c in $o_b z_b$, and the expression is:

$$V_x = \left(V_c - U_{1,t}^L \cos \theta^i(L) + U_{2,t}^L \sin \theta^i(L) \right) \cos \theta_0 - \left(U_{1,t}^L \sin \theta^i(L) + U_{2,t}^L \cos \theta^i(L) \right) \sin \theta_0 \quad (3)$$

$$V_z = \left(V_c - U_{1,t}^L \cos \theta^i(L) + U_{2,t}^L \sin \theta^i(L) \right) \sin \theta_0 + \left(U_{1,t}^L \sin \theta^i(L) + U_{2,t}^L \cos \theta^i(L) \right) \cos \theta_0 \quad (4)$$

Therefore, the boundary condition of the upper end is:

$$MU_{1,t}(L, t) = (F + F_{Dz}) \sin(\theta^i(L) + \theta_0) - Mg \sin \theta^i(L) + F_{Dx} \cos(\theta^i(L) + \theta_0) - P_t (1 + U_{1,s}(L) - \kappa U_2(L)) \quad (5)$$

$$MU_{2,t}(L, t) = (F + F_{Dz}) \cos(\theta^i(L) + \theta_0) - Mg \cos \theta^i(L) - F_{Dx} \sin(\theta^i(L) + \theta_0) - P_t(L) (U_{2,s}(L) + \kappa U_1(L)) \quad (6)$$

When the tethered UAV is in equilibrium, the UAV is stationary in its body coordinate system. The force diagram of the tethered UAV in which the UAV platform is static is shown in Figure 2.

The initial coordinates of the point of tethered UAV are $(s, 0)$, and the coordinates of this point at time t are (x, y) . $x = f(s, t)$, and $y = g(s, t)$. Moreover, the two functions meet the following conditions:

$$\begin{cases} f(s, 0) = s \\ g(s, 0) = 0 \end{cases} \quad (7)$$

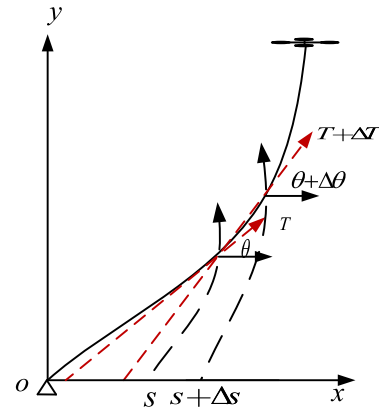


FIGURE 2. Derivation of equations for motion and stress of a tethered UAV.

For the element of tethered UAV, the component of tension at s and $s + \Delta s$ along the x - direction is:

$$T \cos \theta, \quad T \cos \theta + \frac{\partial}{\partial s} (T \cos \theta) \Delta s$$

The component of tension at s and $s + \Delta s$ along the y - direction is:

$$T \sin \theta, \quad T \sin \theta + \frac{\partial}{\partial s} (T \sin \theta) \Delta s$$

From Newton's Law, the following equations are obtained:

$$\rho A \Delta s \frac{\partial^2 x}{\partial t^2} = \frac{\partial (T \cos \theta)}{\partial s} \Delta s \quad (8)$$

$$\rho A \Delta s \frac{\partial^2 y}{\partial t^2} = \frac{\partial (T \sin \theta)}{\partial s} \Delta s \quad (9)$$

A is the cross-sectional area of the cable, and ρ is the density of the cable materials.

Equations (8) and (9) can be simplified as follows:

$$\frac{\partial^2 x}{\partial t^2} = \frac{E}{\rho} \frac{\partial}{\partial s} \left(\frac{\sigma}{E} \cos \theta \right) \quad (10)$$

$$\frac{\partial^2 y}{\partial t^2} = \frac{E}{\rho} \frac{\partial}{\partial s} \left(\frac{\sigma}{E} \sin \theta \right) \quad (11)$$

The Hooke's Law applied to the cable element is:

$$\frac{dS}{ds} = \left[\left(\frac{\partial x}{\partial s} \right)^2 + \left(\frac{\partial y}{\partial s} \right)^2 \right]^{\frac{1}{2}} = \frac{1 + \frac{\sigma}{E}}{1 + \frac{\sigma_0}{E}} \quad (12)$$

Because of

$$\frac{\partial x}{\partial s} = \frac{dS}{ds} \cos \theta, \quad \frac{\partial y}{\partial s} = \frac{dS}{ds} \sin \theta$$

It is observed that

$$\frac{\partial x}{\partial s} = \frac{1 + \frac{\sigma}{E}}{1 + \frac{\sigma_0}{E}} \cos \theta \quad (13)$$

$$\frac{\partial y}{\partial s} = \frac{1 + \frac{\sigma}{E}}{1 + \frac{\sigma_0}{E}} \sin \theta \quad (14)$$

From Equations (10) to (14), the following can be found:

$$\frac{\partial^2}{\partial t^2} \left(\frac{1 + \frac{\sigma}{E}}{1 + \frac{\sigma_0}{E}} \cos \theta \right) = \frac{\partial^2}{\partial s^2} \left(\frac{\sigma}{\rho} \cos \theta \right) \quad (15)$$

$$\frac{\partial^2}{\partial t^2} \left(\frac{1 + \frac{\sigma}{E}}{1 + \frac{\sigma_0}{E}} \sin \theta \right) = \frac{\partial^2}{\partial s^2} \left(\frac{\sigma}{\rho} \sin \theta \right) \quad (16)$$

If the element of the tethered UAV moves parallel to itself, Equations (15) and (16) yield the same condition for the stress σ :

$$\frac{\partial^2 \sigma}{\partial t^2} = \left(1 + \frac{\sigma_0}{E} \right) \frac{E}{\rho} \frac{\partial^2 \sigma}{\partial s^2} \quad (17)$$

The longitudinal wave velocity is:

$$c_l = \sqrt{\left(1 + \frac{\sigma_0}{E} \right) \frac{E}{\rho}} \quad (18)$$

Equations (15) and (16) can be transformed into the following equation:

$$\frac{\partial^2}{\partial t^2} \cos(\theta - \theta_0) = \frac{1 + \frac{\sigma}{E}}{1 + \frac{\sigma_0}{E}} \frac{\sigma}{\rho} \cos(\theta - \theta_0) \quad (19)$$

Here, θ_0 is an arbitrary constant. The transverse wave velocity is:

$$c_t = \sqrt{\frac{1 + \frac{\sigma_0}{E}}{1 + \frac{\sigma}{E}} \frac{E}{\rho}} \quad (20)$$

Moreover, the ratio of transverse wave velocity to longitudinal wave velocity is:

$$\frac{c_t}{c_l} = \left(\frac{\frac{\sigma}{E}}{1 + \frac{\sigma}{E}} \right)^{\frac{1}{2}} \quad (21)$$

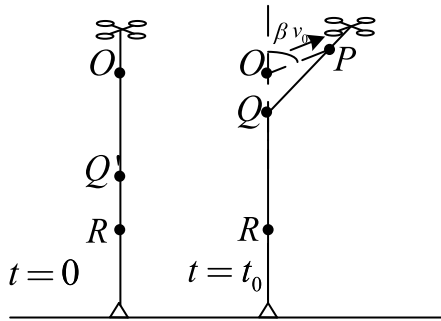


FIGURE 3. Diagram of a tethered UAV due to impact.

Figure 3 shows the diagram of the tethered UAV due to impact. The tethered UAV is left-right symmetrical in the plane; thus, it is only necessary to analyze the impact of the half-plane. The tethered UAV is in equilibrium, and there is prestress σ_0 inside the cable at $t = 0$. At this time, the tethered UAV will be impacted with impact velocity v_0 and impact angle β . At $t = t_0$, the endpoint O of the tethered UAV moves to point P . The transverse wave reaches point Q , and the longitudinal wave reaches point R . After being impacted, the tethered UAV is divided into two linear parts, PQ and RQ , and the rest of R remains in equilibrium. Because the longitudinal wave velocity is greater than the transverse wave velocity, Q obtains the displacement along the β direction, and the particle at R obtains the displacement toward Q . After

the instantaneous displacement, no external force acts on the two particles, moving at a constant speed. Because the cable material is isotropic and the cross-sectional area is constant, the momentum between R and Q is the same at any time; thus, the stress of PQ and RQ is the same and constant. Q' is the point corresponding to Q at time $t = 0$. The geometric relationships between OP , OQ' , and OR are as follows:

$$OP = v_0 t_0, OQ' = c_l t_0, OR = c_l t_0 \quad (22)$$

From $t_1 = \frac{c_t}{c_l} t_0$, the longitudinal wave reaches Q' , and Q' moves toward Q . $t_2 = \left(1 - \frac{c_t}{c_l} \right) t_0$ is the time that Q' reaches Q . Within t_2 , the longitudinal wave is also transmitted from Q' to R . Therefore, the particle velocity of QRu is:

$$u = \frac{\frac{\sigma - \sigma_0}{E}}{1 + \frac{\sigma_0}{E}} c_l \quad (23)$$

The geometric relationship of OQ and PQ

$$OQ = OQ' - QQ' = c_l t_0 - u \left(1 - \frac{c_t}{c_l} \right) t_0 \quad (24)$$

$$PQ = \left[v_0^2 + c_t^2 + u^2 \left(1 - \frac{c_t}{c_l} \right)^2 - 2u \left(1 - \frac{c_t}{c_l} \right) c_t \right]^{\frac{1}{2}} t_0 - \left[+2v_0 c_t \cos \beta - 2v_0 u \left(1 - \frac{c_t}{c_l} \right) \cos \beta \right] t_0 \quad (25)$$

Thus, the elongation of the tethered UAV cable $\varepsilon = PQ - OQ$ at time $t = t_0$ can be obtained:

$$\frac{\varepsilon}{l} = \frac{\varepsilon}{c_l t_0} = \left[v_0^2 + c_t^2 + u^2 \left(1 - \frac{c_t}{c_l} \right)^2 - 2u \left(1 - \frac{c_t}{c_l} \right) c_t + \right]^{\frac{1}{2}} - \frac{c_t - u \left(1 - \frac{c_t}{c_l} \right)}{c_l} \quad (26)$$

According to Hooke's Law, Equation (12) can be found:

$$\frac{1 + \frac{\sigma}{E}}{1 + \frac{\sigma_0}{E}} = \left[v_0^2 + c_t^2 + u^2 \left(1 - \frac{c_t}{c_l} \right)^2 - 2u \left(1 - \frac{c_t}{c_l} \right) c_t \right]^{\frac{1}{2}} - \frac{c_t - u \left(1 - \frac{c_t}{c_l} \right)}{c_l} \quad (27)$$

We introduce $c_0 = (E/\rho)^{\frac{1}{2}}$ and substitute Equations (18), (20), and (23) into Equation (27), and the impact velocity v_0 , impact angle β , and impact stress σ are connected by the relation:

$$\left(\frac{v_0}{c_0} \right) + 2 \frac{v_0}{c_0} \left[\left(\frac{\sigma}{E} \right)^{\frac{1}{2}} \left(1 + \frac{\sigma}{E} \right)^{\frac{1}{2}} - \frac{\sigma - \sigma_0}{E} \right] \cos \beta = 2 \frac{\sigma - \sigma_0}{E} \left(\frac{\sigma}{E} \right)^{\frac{1}{2}} \left(1 + \frac{\sigma}{E} \right)^{\frac{1}{2}} - \left(\frac{\sigma - \sigma_0}{E} \right)^2 \quad (28)$$

TABLE 1. Parameters of the tethered UAV.

| Parameter | Value |
|---|-----------------------------|
| Line density of the cable, ρ | 0.0125 kg/m |
| Cable normal resistance coefficient, C_{dn} | 1.2 m ² |
| Cable length, l | 200 m |
| UAV quality, m | 5.8 kg |
| UAV paddle disc area, A_{pd} | 0.129 m ² |
| Air resistance coefficient of UAV, C_D | 0.064 m ² |
| Cable stiffness, E | 1.867 × 10 ⁹ N/m |
| Cable diameter, d | 0.0034 m |
| Air density, ρ_f | 1.29 kg/m ³ |
| UAV lift coefficient, K_1 | 6.134 × 10 ⁻⁵ |
| UAV rotor speed, Ω_i | 482 rad/s |
| UAV inclination, ϕ | 5° |

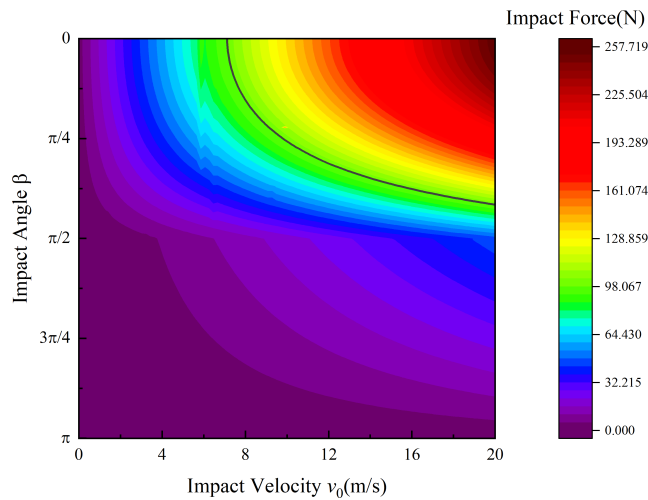


FIGURE 4. Tension distribution of the tethered UAV under different impact velocities and angles.

III. TWO CRITERIA FOR DETERMINING THE DANGEROUS AREA OF TETHERED UAV

Tethered UAV has two types of dangers when operating. First, tethered UAV relies on cables for power supply and has a small-capacity battery. Therefore, broken cable will make the UAV lose power supply and will no longer be actively controlled. Second, when the optical fiber inside the cable is excessively stretched or even broken, the tethered UAV will no longer be able to transmit signals normally. To ensure the normal operation of the tethered UAV, it is necessary to ensure that the maximum tension on the cable during impact is less than its breaking strength. Second, the elongation of the optical fiber should also be less than its allowable elongation. The second criterion does not need to be considered if the first criterion is not satisfied. The breaking strength of the cable is 98.067 N, and the maximum elongation does not exceed 0.5% [17]. The dangerous area of tethered UAV operation is studied based on these two criteria.

The parameters of the tethered UAV according to [25] are listed in Table 1. The tethered UAV will be in danger when the impact velocity and angle reach a certain value. At this time, the value beyond this range is a dangerous area for

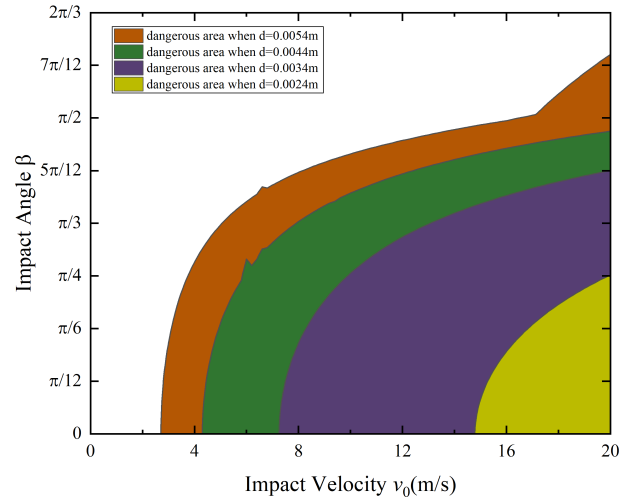


FIGURE 5. The dangerous area of tethered UAVs with different diameters.

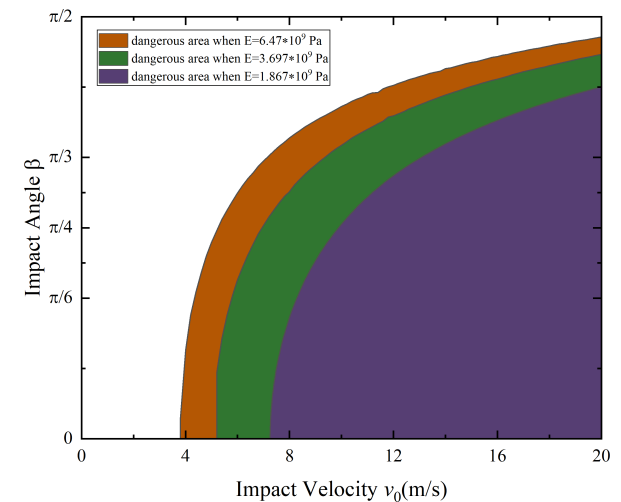


FIGURE 6. The dangerous area of the tethered UAV with elastic modulus.

the tethered UAV. To determine the dangerous area for the tethered UAV under different impact velocities and impact angles, it is imperative to determine the tethered UAV's dynamic response and analyze it in combination with two failure criteria.

IV. NUMERICAL RESULTS FOR THE DANGEROUS AREA
A. DETERMINATION OF THE DANGEROUS AREA BASED ON THE BREAKING STRENGTH

The tension distribution of the tethered UAV under different impact velocities and different impact angles is shown in Figure 4. It is observed that the smaller is the impact angle, the greater is the impact force, and the greater is the impact velocity, the greater is the impact force. The black contour line represents the tension of 98.067 N. The part whose value is greater than the black contour is the dangerous area. The intersections of the black contour and the upper and right axes represent the critical value of the dangerous area for the tethered UAV when the impact angle is minimal and the impact velocity is maximal, respectively. When the impact

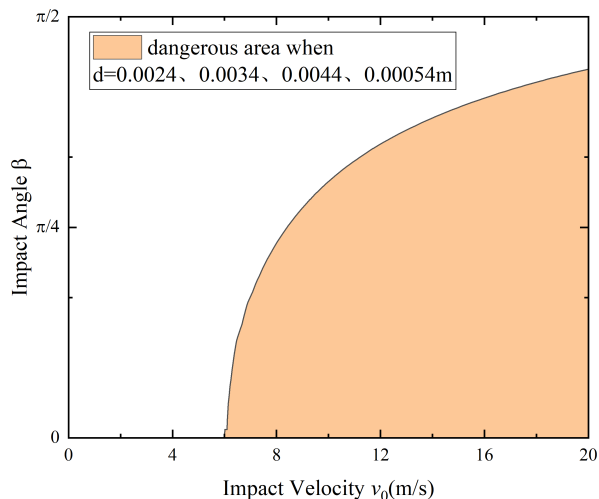


FIGURE 7. The dangerous area of tethered UAVs with different diameters based on the second criterion.

velocity reaches 7.25 m/s and the impact angle is 0, the cable begins to break. When the impact velocity reaches 20 m/s and the impact angle is $5/6 \pi$, the cable will also be broken, and the tethered UAV is in a dangerous area.

The cable’s cross-section determines the transmission power and influences the impact force. The dangerous area of the tethered UAV within the diameter range from 0.0024 m to 0.0054 m is shown in Figure 5.

It is observed that with the continuous increase in cable diameter, the dangerous area of the tethered UAV also increases. When the cable diameters are 0.0024, 0.0034, and 0.0044 m, even if the impact velocity reaches the maximum, as long as the impact angle is less than $\pi/2$, the tethered UAV is still in the safe working area. However, when the cable diameter is 0.0054 m and the impact velocity is greater than 16.56 m/s, the tethered UAV will still be in the danger area even if the impact angle is greater than $\pi/2$.

The dangerous area of the tethered UAV under different elastic moduli based on the cable breaking strength is shown in Figure 6. It is observed that with the increase in the elastic modulus, the dangerous area of the tethered UAV also increases.

B. DETERMINATION OF THE DANGEROUS AREA BASED ON THE MAXIMUM ELONGATION

The dangerous area of the tethered UAV under different cable diameters based on the maximum elongation of the optical fiber is shown in Figure 7. It is observed that the different diameters of the cable have no clear effect on the elongation of the optical fiber. Under this condition, cables with a larger cross-sectional area should be selected because a larger cross-sectional area can accommodate more optical fibers, which is beneficial to signal transmission.

The dangerous area of the tethered UAV under different elastic moduli based on the maximum elongation of the optical fiber is shown in Figure 8. It is observed that with the continuous increase in the elastic modulus, the dangerous area of

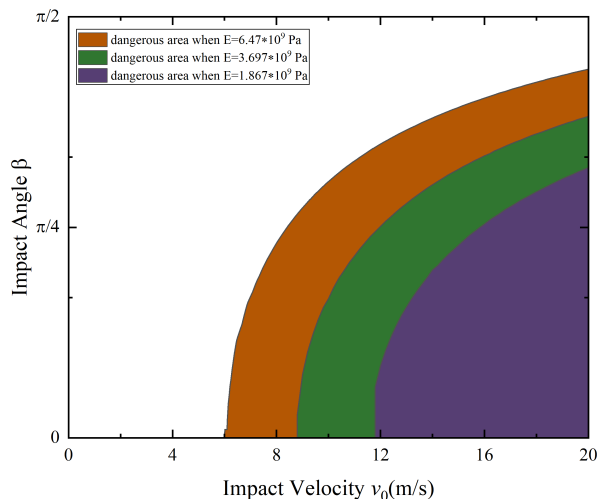


FIGURE 8. The dangerous area of the tethered UAV with an elastic modulus based on the second criterion.

the tethered UAV increases. Compared with Figure 6, under the same Young’s modulus, the dangerous area of the tethered UAV based on the maximum elongation of the optical fiber is smaller. This shows that when the impact speed and angle do not break the cable, the elongation of the optical fiber will be less than its maximum elongation.

V. ENGINEERING SUGGESTION

- 1) To ensure the normal operation of the tethered UAV, cables with a smaller elastic modulus and smaller cross-sectional area should be selected.
- 2) Whether the tethered UAV will fail when it is impacted shall be judged mainly according to the breaking strength of the cable.
- 3) According to [17], the average wind speed in the South China Sea is 5~7 m/s, and the maximum wind speed is 20 m/s. When the active control of the UAV is ignored, as the wind speed suddenly changes, the speed of the UAV will not be greater than the wind speed in a short time. Currently, the qualified elastic modulus and diameter are 1.867×10^9 N/m and 0.0024 and 0.0034 m, respectively. At the same time, because a larger cross-sectional area of the cable can accommodate more optical fibers and provide more power, the cable with an elastic modulus of 1.867×10^9 N/m and a diameter of 0.0034 m should be used.

VI. CONCLUSION

Starting with the impact stress of the tethered UAV under impact, this study analyzes the impact angle and impact velocity on the tethered UAV. Combined with the two failure criteria of the tethered UAV, the range of danger areas of tethered UAVs under different working conditions is given. It was found that cables with a smaller elastic modulus and smaller cross-sectional areas should be selected to ensure the normal operation of the tethered UAV, and whether the tethered UAV will fail when it is impacted will be judged mainly according to the breaking strength of the cable. Combined

with the actual working range of the tethered UAV, taking the tethered UAV working in the South China Sea as an example, the safest material parameters of the tethered UAV are given to ensure its normal operation.

Compared with previous research on the damage caused by the impact of ordinary UAVs, this study focuses on the impact of cables on tethered UAVs. This is important because, in actual operation, the cable is often impacted. If the cable fails, the whole tethered UAV will not operate normally. In the future, further research will be conducted on the response of the tethered UAV when facing impact in more complex environments. For example, ship-borne tethered UAVs face end impacts (caused by ship motion) and multiple loads of wind, waves, and currents. The corresponding tethered UAV parameter range and engineering suggestions will be given to ensure its normal operation.

REFERENCES

- [1] H.-F. Wang, L. Zhai, H. Huang, L.-M. Guan, K.-N. Mu, and G.-P. Wang, "Measurement for cracks at the bottom of bridges based on tethered creeping unmanned aerial vehicle," *Autom. Construct.*, vol. 119, Nov. 2020, Art. no. 103330.
- [2] C. Viegas, B. Chehreh, J. Andrade, and J. Lourenço, "Tethered UAV with combined multi-rotor and water jet propulsion for forest fire fighting," *J. Intell. Robot. Syst.*, vol. 104, no. 2, pp. 1–13, Feb. 2022.
- [3] Z. Xu, *Application Research of Tethered UAV Platform in Marine Emergency Communication Network*. Copenhagen, Denmark: River Publishers, 2021.
- [4] C. Chen, Y. Guo, J. Liu, J. Yu, and F. Raza, "Research on dropping test and numerical simulation for unmanned aerial vehicle," *Int. J. Crashworthiness*, vol. 27, no. 1, pp. 1–17, 2021.
- [5] A. K. Jha, S. Sathyamoorthy, and V. Prakash, "Bird strike damage and analysis of UAV's airframe," *Proc. Struct. Integrity*, vol. 14, pp. 416–428, Jan. 2019.
- [6] X. Lu, X. Liu, Y. Zhang, Y. Li, and H. Zuo, "Simulation of airborne collision between a drone and an aircraft nose," *Aerosp. Sci. Technol.*, vol. 118, Nov. 2021, Art. no. 107078.
- [7] Y. Zhang, Y. Huang, K. Liang, K. Cao, Y. Wang, X. Liu, Y. Guo, and J. Wang, "High-precision modeling and collision simulation of small rotor UAV," *Aerosp. Sci. Technol.*, vol. 118, Nov. 2021, Art. no. 106977.
- [8] E. T. Campollettano, M. L. Bland, R. A. Gellner, D. W. Sproule, B. Rowson, A. M. Tyson, S. M. Duma, and S. Rowson, "Ranges of injury risk associated with impact from unmanned aircraft systems," *Ann. Biomed. Eng.*, vol. 45, no. 12, pp. 2733–2741, Dec. 2017.
- [9] X. Meng, Y. Sun, J. Yu, Z. Tang, J. Liu, T. Suo, and Y. Li, "Dynamic response of the horizontal stabilizer during UAS airborne collision," *Int. J. Impact Eng.*, vol. 126, pp. 50–61, Apr. 2019.
- [10] C. H. Koh, K. Low, L. Li, Y. Zhao, C. Deng, S. K. Tan, Y. Chen, B. C. Yeap, and X. Li, "Weight threshold estimation of falling UAVs (Unmanned Aerial Vehicles) based on impact energy," *Transp. Res. C, Emerg. Technol.*, vol. 93, pp. 228–255, Aug. 2018.
- [11] H. Liu, M. H. C. Man, and K. H. Low, "UAV airborne collision to manned aircraft engine: Damage of fan blades and resultant thrust loss," *Aerosp. Sci. Technol.*, vol. 113, Jun. 2021, Art. no. 106645.
- [12] W. Yang, "Design and control algorithm for moored ship-borne unmanned aerial vehicle with large load," M.S. thesis, Dept. Astron. Eng., Harbin Inst. Technol., Harbin, China, 2018.
- [13] M. M. Nicotra, R. Naldi, and E. Garone, "Nonlinear control of a tethered UAV: The taut cable case," *Automatica*, vol. 78, pp. 174–184, Apr. 2017.
- [14] F. Muttin, "Umbilical deployment modeling for tethered UAV detecting oil pollution from ship," *Appl. Ocean Res.*, vol. 33, no. 4, pp. 332–343, Oct. 2011.
- [15] Y. Liu, F. Zhang, P. Huang, and X. Zhang, "Analysis, planning and control for cooperative transportation of tethered multi-rotor UAVs," *Aerosp. Sci. Technol.*, vol. 113, Jun. 2021, Art. no. 106673.
- [16] K. Talke, F. Birchmore, and T. Bewley, "Autonomous hanging tether management and experimentation for an unmanned air-surface vehicle team," *J. Field Robot.*, vol. 39, no. 6, pp. 869–887, Sep. 2022.
- [17] W. He and S. Zhang, "Stability parameter range of a tethered unmanned aerial vehicle," *Shock Vib.*, vol. 2022, pp. 1–13, Jan. 2022.
- [18] O. M. Bushnaq, M. A. Kishk, A. Celik, M.-S. Alouini, and T. Y. Al-Naffouri, "Optimal deployment of tethered drones for maximum cellular coverage in user clusters," *IEEE Trans. Wireless Commun.*, vol. 20, no. 3, pp. 2092–2108, Mar. 2020.
- [19] A. Kourani and N. Daher, "Marine locomotion: A tethered UAV-buoy system with surge velocity control," *Robot. Auto. Syst.*, vol. 145, Nov. 2021, Art. no. 103858.
- [20] L. A. Sandino, D. Santamaria, M. Bejar, A. Viguria, K. Kondak, and A. Ollero, "Tether-guided landing of unmanned helicopters without GPS sensors," in *Proc. IEEE Int. Conf. Robot. Autom. (ICRA)*, May 2014, pp. 3096–3101.
- [21] U. Starossek, "Disproportionate collapse: A pragmatic approach," *Struct. Buildings*, vol. 160, no. 6, pp. 317–325, Dec. 2007.
- [22] U. Starossek, "Collapse resistance and robustness of bridges," in *Proc. 4th Int. Conf. Bridge Maintenance, Saf. Manage.*, Seoul, South Korea, 2018, pp. 13–17.
- [23] T. P. Zoli and J. Steinhouse, "Some considerations in the design of long span bridges against progressive collapse," in *Proc. 23rd U.S.-Jpn. Bridge Eng. Workshop*, 2007, pp. 4–11.
- [24] R. Judge, Z. Yang, S. W. Jones, G. Beattie, and I. Horsfall, "Spiral strand cables subjected to high velocity fragment impact," *Int. J. Impact Eng.*, vol. 107, pp. 58–79, Sep. 2017.
- [25] P. G. Ioppo, "The design, modeling and control of an autonomous tethered multirotor UAV," M.S. thesis, Univ. Stellenbosch, Stellenbosch, South Africa, 2017.



TAO YE received the master's degree in mechanics from Tianjin University, China. He has a good mechanical foundation and in his master's thesis, he used the stress wave method to study the complicated dynamic response of the ship-borne tethered UAV under lower-end excitation. His research interests include aerospace, nonlinear dynamics, ocean engineering, and acoustics. He focuses on the vibration and dynamic behaviors of the tethered UAV under wind load and ship oscillation.



XU XIANGYU received the master's degree from Tianjin University, Tianjin, China, in 2022. He is currently pursuing the doctoral degree in civil engineering with the Institute of Defense Engineering, AMS, PLA, Beijing, China. His interests include defense engineering and dynamics.



DAI JIAXI received the master's degree from Shenyang Jianzhu University. She is a Researcher with Shenyang Urban Construction University. Her research interests include structural safety and structural dynamics.

...